Two color delay dependent IR probing
of torsional isomerization in a [AgL₁L₂]⁺ complex

Johannes Lang, Maximilian Gaffga, Fabian Menges

and Gereon Niedner-Schatteburg

*Fachbereich Chemie and Forschungszentrum OPTIMAS,
Technische Universität Kaiserslautern,
67663 Kaiserslautern, Germany*

Two color infrared multiple photon dissociation (2c-IR-MPD) spectroscopy with delayed pulses indicate a torsional isomerization in a "ligand-metal-chelate" complex $[AgL_1L_2]^+$. *Ab initio* calculations reveal the torsional barrier as well as the change of vibrational frequencies and IR intensities along the isomerization pathway. The current approach bears prospects for further elucidation of competing interactions within naked or microsolvated complexes in gas phase coordination chemistry.

Metal ions stabilize through reversible solvation or persistent coordination. In appropriate mixtures ligand exchange drives equilibria towards the formation of complexes with as many strongly coordinating ligands as possible within steric and electronic constraints.

Mass produced chelating agents like ethylenediaminetetraacetic acid (EDTA)[1] serve in the extraction of heavy metal ions from waste waters and in alkaline earth metal ion scavenging for water softening on a large scale[2, 3]. Environmental issues[4] call for biodegradability (as e.g. fulfilled by Trilon M®[5, 6]) and for further optimization of the chelation processes[7]. The finely tuned interplay between ligand to ligand and ligand to solvent interaction (including hydrogen bonding) plays a crucial role in the reversible stabilization of metal ions within such chelated complexes[8, 9]. It is paramount to acquire insight into their structure and vibrational dynamics in order to advance our understanding of the dominating processes and the prevailing equilibria.

The combination of mass spectrometry with infrared (IR) laser spectroscopy is suitable for the characterization of stoichiometrically defined coordination complexes, and recent two color double resonance studies proved instrumental to obtain isomer sensitivity of various gas phase complexes and clusters[10-14]. Experimental spectra taken in such solvent free environments correspond to *ab initio* calculations of isolated species, thus yielding insight into the structure and dynamics of likely binding motifs. We have recently applied a two color IR-MPD detection scheme to study an isolated di-nuclear silver complex which spontaneously forms in solution by coordination with nucleobase mimicking ligands[15].

Here, we investigate a flexible arrangement of a single Ag(I) center with two coordinating ligands, α-Cyano-4-hydroxycinnamic acid (HCCA = L_1, monodentate ligand) and 2-(5-methyl-1H-pyrazol-3-yl)pyridine[16] (MPP = L_2, bidentate chelate), one each. The resulting $[AgL_1L_2]^+$ complex serves as a model for a ligand to chelate hydrogen bonding within a "ligand-metal-chelate" complex. A possible torsional isomerization (cf. Scheme 1) is the subject of verification and characterization by this study.

<div align="center">

Scheme 1

</div>

A sample solution of $AgNO_3$, HCCA and MPP[17] in acetonitrile at concentrations of 1 x 10^{-5} M was used without further purification and continuously infused into an electrospray ion trap instrument (Bruker amaZon SL, cf. Supplement for further experimental details). We

deduced the formation of the self-assembled $[AgL_1L_2]^+$ complex from the recording of a cation signal at m/z = 455 and 457 (due to the ^{107}Ag and ^{109}Ag isotopes). The isotopic pattern clearly proves a complexation of a Ag(I) ion (cf. Fig. S-1, middle inset) by neutral L_1 and L_2 ligands leading to a singly charged ligand-metal-chelate complex. Collision induced dissociation inside the ion trap exhibits the exclusive loss of the monodentate L_1 ligand (cf. Fig. S-1, top inset).

We employed IR-MPD spectroscopy in the 1200 – 3800 cm^{-1} range on the $[AgL_1L_2]^+$ complex (cf. top of Fig. 1) using a tunable high power OPO/OPA IR laser (IR$_{scan}$, LaserVision, cf. SI.2 and SI.3 for further experimental details). The observed bands can be assigned by comparison to DFT derived vibrational spectra: OH stretching vibration of the phenolic OH group ($\tilde{v}_{Ph\underline{OH}}$ = 3639 cm^{-1}), OH stretching vibration of the carboxyl group ($\tilde{v}_{CO\underline{OH}}$ = 3581 cm^{-1}), free NH stretching vibration of the L_2 chelate ($\tilde{v}_{NH}$ = 3490 cm^{-1}) and hydrogen bonded NH stretching vibration of the L_2 chelate ($\tilde{v}_{NH}^{H-bound}$ around 3400 cm^{-1}), aliphatic CH stretching vibrations ($\tilde{v}_{CH}^{aliph.}$ around 2960 cm^{-1}), C=C vibrations ($\tilde{v}_{C=C}$ = 1600 cm^{-1}) as well as carboxylic CO stretching band in L_1 ($\tilde{v}_{\underline{CO}OH}$ around 1780 cm^{-1}). A spurious dip in the $\tilde{v}_{Ph\underline{OH}}$ band at 3630 cm^{-1} is an artefact of known fluctuations in the IR$_{scan}$ laser power. The simultaneous occurrence of a free and a hydrogen bonded NH stretching vibration cannot result from a single isomer, since there is only one NH group in the $[AgL_1L_2]^+$ complex. This indicates the coexistence of at least two isomers in the gas phase. The $\tilde{v}_{CO\underline{OH}}$ band at 3581 cm^{-1} is red shifted with respect to the calculation which explains by a higher anharmonicity of the carboxylic $\tilde{v}_{CO\underline{OH}}$ relative to the phenolic $\tilde{v}_{Ph\underline{OH}}$ [18-20].

Figure 1

Minimum energy structures, relative energies and linear IR spectra were calculated at the B3LYP[21-24]/cc-pVTZ[25] level of theory as implemented in the Gaussian 09 program package[26]. The Stuttgart-Dresden effective core potential basis set was used to represent the Ag atom[27]. Harmonic vibrational frequencies were scaled by the factor 0.96 (1.0) for the stretching modes above (below) 2000 cm^{-1} to match the most intense experimental bands (e.g. $\tilde{v}_{Ph\underline{OH}}$ at 3639 cm^{-1}). Calculated intensities were multiplied by the photon energy (in cm^{-1}) for normalization. We found at least four energetically favored coordination motifs in $[AgL_1L_2]^+$ (cf. Fig. 1, structures A-D). Structure A is the energetically most favorable. Energies of structures B-D are given relative to the energy of structure A. Within the

structures A and B, the silver ion is coordinated by the nitrile group of the L_1 ligand and two nitrogen atoms of the L_2 chelate. Structure A allows for the formation of a NH---O hydrogen bond (d($\underline{N}$H---$\underline{O}$) = 3.011 Å, d(N$\underline{H}$---$\underline{O}$) = 2.035 Å) between the NH group of L_2 and the carboxyl group of L_1. Structures A and B are rotational conformers, where L_1 and L_2 twist against each other by about 180°. This rotation allows for the formation of a new CH---O hydrogen bond (d($\underline{C}$H---$\underline{O}$) = 4.058 Å, d(C$\underline{H}$---$\underline{O}$) = 2.989 Å) between a pyridine CH in L_2 and the carboxyl group of L_1. The computed bond distances are only slightly above typical values of similar bands in the solid state[28]. Nevertheless, the CH---O hydrogen bonded structure B is less stable by 8 kJ/mol than the NH---O hydrogen bonded structure A. In isomers C and D, the silver ion is coordinated by the same two nitrogen atoms of L_2 as in A and B, whereas - from the L_1 point of view - the terminal oxygen atom of the carboxyl group serves as electron donor in C and D, instead of the nitrile group in isomers A and B. A mere rotation by 180° transfers structure C (21 kJ/mol) into structure D (33 kJ/mol), which makes them mutual rotamers.

The experimental one color IR-MPD spectrum can be explained by a mixture of isomers A and B. There is no evidence of isomers C and D, which would exhibit a red shifted CO stretching vibration due to the coordination of the Ag(I) ion by the terminal carboxyl oxygen atom. The $\tilde{v}_{Ph\underline{OH}}$ and $\tilde{v}_{CO\underline{OH}}$ bands, corresponding to free OH and COOH stretching motions, result from both isomers A and B. The hydrogen bonded NH stretching vibration $\tilde{v}_{NH}^{H-bound}$ exclusively results from isomer A, while the NH stretching band $\tilde{v}_{NH}$ is indicative of isomer B. The predicted intensity of $\tilde{v}_{NH}^{H-bound}$ is much higher than observed, which is a known finding in hydrogen bonding that broadens and smears out the affected vibrations. Observed bands in the CO stretching region around 1800 cm^{-1} correlate well to those of isomers A and B. The recorded spectra do not reveal the predicted strong bands (around 1640 - 1650 cm^{-1}) of the high energy isomers C and D. It is a pending task to record two color IR-MPD spectra in the fingerprint region below 2000 cm^{-1} and to perform an in detail interpretation. It is warranted already at this stage, however, that the current findings on [AgL$_1$L$_2$]$^+$ conclude in the coexistence of isomers A and B in most likely absence of C and D.

Figure 2

We investigated by further DFT calculations the torsional conversion of isomers A to B through parametrical variation of an appropriate dihedral angle (between $H^1Ag^2N^3O^4$, cf. scheme 1), which can be thought of as the intersection angle of the two planes spanned by atoms $H^1Ag^2N^3$ and $Ag^2N^3O^4$. Our calculations performed full structural relaxation at fixed dihedral angles in steps of 10° with closer intervals of 4° around the minima at 0° and 180° in order to extract pointwise values of relative energies, vibrational frequencies and IR intensities (cf. Fig. 2, from bottom to top).

Isomers A and B are well confirmed by the energetic minima at 0° and 180° (cf. Fig. 2, right, bottom), and we find a higher (lower) torsional stiffness in the OH (CH) hydrogen bonded more (less) stable isomer A (B) with a torsional barrier of 12 kJ/mol. The majority of vibrational modes is decoupled from the torsional isomerization and their frequencies persist without significant change at the geometries of isomers A and B and – most notably – at all dihedral angles in between. However, there are considerable red shifts of those vibrational bands that are involved in hydrogen bonding, and concomitant variations of their IR intensities. At a dihedral angle of 0°, isomer A is the favorable structure and $\tilde{v}_{NH}^{H-bound}$ is red shifted due to the hydrogen bond and its IR intensity is strongly enhanced. At 180 °, isomer B, the pyridinic CH group is involved in a CH---O hydrogen bond. There are at least four IR active normal modes of the pyridine ring that involve this CH group. We chose to plot the mode with the strongest change of IR intensities (cf. Fig. S-2 for its definition and Fig. S-3 for torsional plots of IR intensity changes in other CH stretching modes). Its frequency shifts slightly to the red upon hydrogen bonding while its IR intensity increases considerably. All findings of the parametric torsional variation nicely confirm strong NH---O hydrogen bonding in isomer A and weak CH---O hydrogen bonding in isomer B.

Figure 3a) and 3b)

In order to investigate the predicted interconversion of isomers A and B experimentally, we applied the two color IR-MPD technique to the $[AgL_1L_2]^+$ complex. An attenuated IR laser (IR$_{fix}$) is set resonant to $\tilde{v}_{Ph\underline{OH}}$ at 3639 cm^{-1}, and a high power scanning IR laser (IR$_{scan}$) was used to measure delay dependent IR-MPD spectra (cf. Fig. 3a)). The time delay Δt between the two laser pulses (6 ns each) is defined as:

$$\Delta t = t\big(IR_{fix}\big) - t\big(IR_{scan}\big) \qquad (1)$$

It depends on the time delay Δt between the IR_{scan} and IR_{fix} pulses whether the hydrogen bound NH stretching band around 3400 cm^{-1} is observable or not. Note, that the application of a second laser pulse causes some increase of the baselines in the two color IR-MPD spectra as compared to the one color spectrum.

When the IR_{scan} pulse excites the $[AgL_1L_2]^+$ complex ahead of the IR_{fix} pulse (Δt positive, red line spectrum in Fig. 3a)) then there is some increase in IR-MPD fragmentation yield with respect to the one color spectrum (black curve) on all bands. In this case the IR_{fix} pulse serves to enhance the absolute fragmentation yield. It does not, however, alter the isomer population as recorded by the one color experiment. The two color spectrum thus probes "cold" (here: room temperature) complexes. In particular, the hydrogen bonded NH vibration ($\tilde{v}_{NH}^{H-bound}$) becomes strongly enhanced and clearly observable.

However, when the time delay reverses (Δt negative, blue curve in Fig. 3a), such that the IR_{fix} pulse excites first, the IR-MPD yield of $\tilde{v}_{NH}^{H-bound}$ diminishes and the intensity of $\tilde{v}_{NH}$, the free NH vibration, increases with respect to the two color IR-MPD spectrum with positive Δt. A pointwise scan of Δt reveals a fast switch amongst both vibrations (cf. Fig. 3b). We interpret this finding as follows: Firstly, the IR_{fix} laser heats the complexes and induces an isomerization such that the population of isomer A (evidenced by the hydrogen bonded $\tilde{v}_{NH}^{H-bound}$ vibration) is diminished and the population of isomer B (free $\tilde{v}_{NH}$ vibration) is enhanced. The possibility of some isomers at skewed dihedral angles, which are void of any L_1 to L_2 bonding, is acknowledged; present results do not find any evidence, however. Subsequently, the changed isomer population is detected by the IR_{scan} laser. This interpretation matches the observation of a significant broadening and red shifting of the three recorded stretching vibrations, as known to occur from a rovibrational preheating of part of the $[AgL_1L_2]^+$ ensemble by the IR_{fix} pulse – prior to the scanning IR_{scan} pulse.

Our study revealed that strong and weak hydrogen bonds[29-31] within the given complex may break and form by torsional rearrangments that take place perpendicular to the hydrogen bond directions (here, through torsional twisting of the two ligands against each other). It confirms that the forming and breaking of hydrogen bonds is of a multi dimensional character – much beyond an intuitive pulling apart of a hydrogen bond along its bond

direction. It further elucidates how weak CH---O hydrogen bonds may come into play to stabilize conformers other than the global minimum structure. The importance of torsional rearrangements becomes clear once more by the gained picture, as was e.g. similarly unravelled in a previous study on intra ligand torsionin a Ru complex that precedes and enables activation of the catalytic center in a somewhat surprising way[16]. Our studies benefit from two color IR pulse probing as a valuable tool for such investigations (two color IR-MPD). Variable time delays between the two laser pulses allow to probe ion ensembles with variable internal energy. The preheating effect of the additional IR_{fix} pulse could be demonstrated in terms of laser induced torsional isomerization as well as a red shifting and broadening of the IR-MPD bands. The torsional isomerization path was examined by concomitant DFT calculations that served to elucidate the torsional barrier, the relative stabilities of participating isomers, and the change of vibrational frequencies and IR intensities in the course of formation and breaking of strong and weak hydrogen bonds amongst chelate and ligand in a semi flexible ligand-metal-chelate complex.

The present study presents work in progress. Δt tuning two color IR-MPD spectra of the $\tilde{v}_{CH}^{aliph.}$ range (around 3000 cm^{-1}) and in the fingerprint region (below 2000 cm^{-1}) as well as temperature dependent measurements will help to provide more insight into the details of population dynamics in the $[AgL_1L_2]^+$ model system. Further complexes are to follow in order to learn more about the competing interactions of strong coordination and weak auxiliary bonds in multiple coordinated metal complexes.


Acknowledgement

References

1.   M. S. Vohra, *International Journal of Environmental Science and Technology*, 2010, **7**, 687-696.
2.   L. Suarez, M. A. Diez, R. Garcia and F. A. Riera, *Separation and Purification Technology*, 2013, **118**, 144-150.
3.   D. Kołodyńska, *Desalination*, 2011, **267**, 175-183.
4.   P. Römkens, L. Bouwman, J. Japenga and C. Draaisma, *Environmental Pollution*, 2002, **116**, 109-121.
5.   J. Jachuła, D. Kołodyńska and Z. Hubicki, *Chemical Engineering Research and Design*, 2012, **90**, 1671-1679.
6.   J. Jachuła, D. Kołodyńska and Z. Hubicki, *cent.eur.j.chem.*, 2011, **9**, 52-65.
7.   P. Muller, in *Pure and Applied Chemistry*, 1994, vol. 66, p. 1077.
8.   B. Zhao, Z. Han and K. Ding, *Angewandte Chemie International Edition*, 2013, **52**, 4744-4788.
9.   K. Biradha, G. R. Desiraju, D. Braga and F. Grepioni, *Organometallics*, 1996, **15**, 1284-1295.
10.   C. M. Leavitt, A. B. Wolk, J. A. Fournier, M. Z. Kamrath, E. Garand, M. J. Van Stipdonk and M. A. Johnson, *The Journal of Physical Chemistry Letters*, 2012, **3**, 1099-1105.
11.   T. R. Rizzo, J. A. Stearns and O. V. Boyarkin, *International Reviews in Physical Chemistry*, 2009, **28**, 481-515.
12.   A. Fujii and K. Mizuse, *International Reviews in Physical Chemistry*, 2013, **32**, 266-307.
13.   N. Heine, M. R. Fagiani, M. Rossi, T. Wende, G. Berden, V. Blum and K. R. Asmis, *Journal of the American Chemical Society*, 2013, **135**, 8266-8273.
14.   K. Tanabe, M. Miyazaki, M. Schmies, A. Patzer, M. Schutz, H. Sekiya, M. Sakai, O. Dopfer and M. Fujii, *Angewandte Chemie-International Edition*, 2012, **51**, 6604-6607.
15.   Y. Nosenko, F. Menges, C. Riehn and G. Niedner-Schatteburg, *Physical Chemistry Chemical Physics*, 2013, **15**, 8171-8178.
16.   L. Taghizadeh Ghoochany, C. Kerner, S. Farsadpour, F. Menges, Y. Sun, G. Niedner-Schatteburg and W. R. Thiel, *European Journal of Inorganic Chemistry*, 2013, **2013**, 4305-4317.
17.   K. Muller, Y. Sun, A. Heimermann, F. Menges, G. Niedner-Schatteburg, C. van Wüllen and W. R. Thiel, *Chemistry – A European Journal*, 2013, **19**, 7825-7834.
18.   G. M. Florio, T. S. Zwier, E. M. Myshakin, K. D. Jordan and E. L. Sibert, *The Journal of Chemical Physics*, 2003, **118**, 1735-1746.
19.   J. L. Leviel and Y. Marechal, *The Journal of Chemical Physics*, 1971, **54**, 1104-1107.
20.   J. Antony, G. von Helden, G. Meijer and B. Schmidt, *The Journal of Chemical Physics*, 2005, **123**, -.
21.   A. D. Becke, *Physical Review A*, 1988, **38**, 3098-3100.
22.   C. T. Lee, W. T. Yang and R. G. Parr, *Phys Rev B*, 1988, **37**, 785-789.
23.   B. Miehlich, A. Savin, H. Stoll and H. Preuss, *Chem Phys Lett*, 1989, **157**, 200-206.
24.   A. D. Becke, *J Chem Phys*, 1993, **98**, 5648-5652.
25.   T. H. Dunning, *J Chem Phys*, 1989, **90**, 1007-1023.
26.   M. J. Frisch, G. W. Trucks, H. B. Schlegel, G. E. Scuseria, M. A. Robb, J. R. Cheeseman, G. Scalmani, V. Barone, B. Mennucci, G. A. Petersson, H. Nakatsuji, M. Caricato, X. Li, H. P. Hratchian, A. F. Izmaylov, J. Bloino, G. Zheng, J. L. Sonnenberg, M. Hada, M. Ehara, K. Toyota, R. Fukuda, J. Hasegawa, M. Ishida, T. Nakajima, Y. Honda, O. Kitao, H. Nakai, T. Vreven, J. A. Montgomery, J. E. Peralta, F. Ogliaro, M. Bearpark, J. J. Heyd, E. Brothers, K. N. Kudin, V. N. Staroverov, R. Kobayashi, J. Normand, K. Raghavachari, A. Rendell, J. C. Burant, S. S. Iyengar, J. Tomasi, M. Cossi, N. Rega, J. M. Millam, M. Klene, J. E. Knox, J. B. Cross, V. Bakken, C. Adamo, J. Jaramillo, R. Gomperts, R. E. Stratmann, O. Yazyev, A. J. Austin, R. Cammi, C. Pomelli, J. W. Ochterski, R. L. Martin, K. Morokuma, V. G. Zakrzewski, G. A. Voth, P. Salvador, J. J. Dannenberg, S. Dapprich, A. D. Daniels, Farkas, J. B. Foresman, J. V. Ortiz, J. Cioslowski and D. J. Fox, Wallingford CT, 2009.

27.   M. Dolg, H. Stoll, H. Preuss and R. M. Pitzer, *The Journal of Physical Chemistry*, 1993, **97**, 5852-5859.
28.   G. R. Desiraju, *Accounts of Chemical Research*, 1991, **24**, 290-296.
29.   I. Rozas, *Physical Chemistry Chemical Physics*, 2007, **9**, 2782-2790.
30.   E. Arunan, G. R. Desiraju, R. A. Klein, J. Sadlej, S. Scheiner, I. Alkorta, D. C. Clary, R. H. Crabtree, J. J. Dannenberg, P. Hobza, H. G. Kjaergaard, A. C. Legon, B. Mennucci and D. J. Nesbitt, *Pure and Applied Chemistry*, 2011, **83**, 1619-1636.
31.   E. Arunan, G. R. Desiraju, R. A. Klein, J. Sadlej, S. Scheiner, I. Alkorta, D. C. Clary, R. H. Crabtree, J. J. Dannenberg, P. Hobza, H. G. Kjaergaard, A. C. Legon, B. Mennucci and D. J. Nesbitt, *Pure and Applied Chemistry*, 2011, **83**, 1637-1641.

Figures and captions
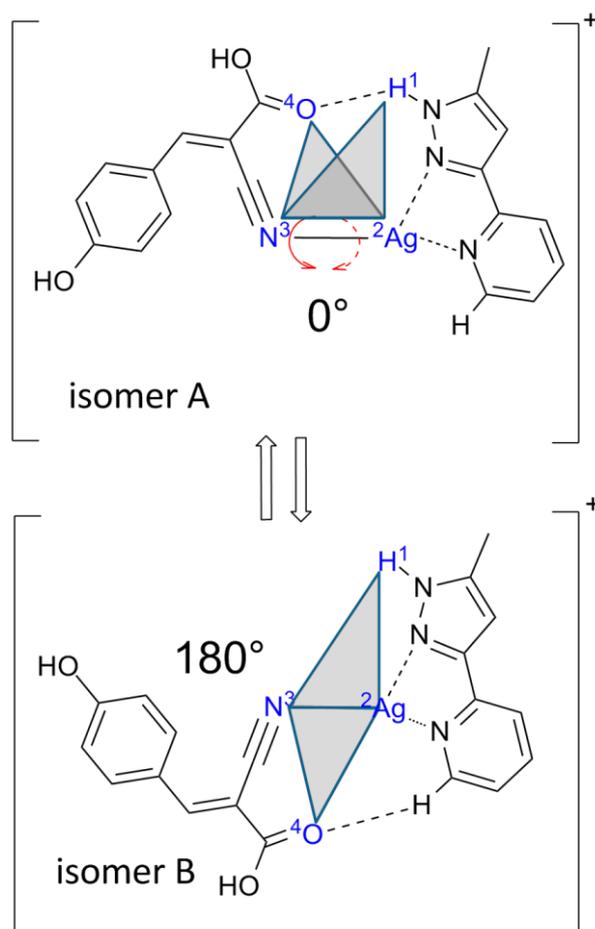
Scheme 1: Definition of the dihedral angle that describes the torsional isomerization in the $[AgL_1L_2]^+$ complex. Note, that isomer A stabilizes through a NH---O hydrogen bond and isomer B through a CH---O hydrogen bond.
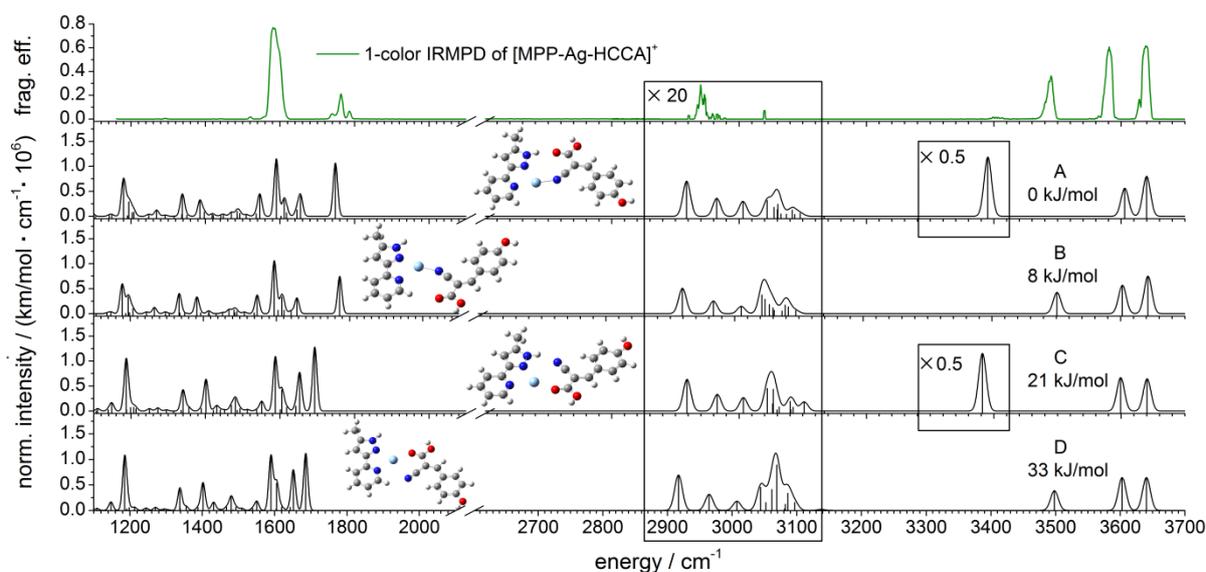
Figure 1): IR-MPD spectrum of the $[AgL_1L_2]^+$ complex (green, L_1 loss recorded) in comparison with the DFT calculations at the B3LYP/cc-pVTZ (H, C, N, O) and Stuttgart 1997 ECP (Ag) level of theory (black). Frequencies are scaled with 0.96 (1.0) above (below) 2000 cm^{-1}. Intensities are multiplied by the photon energy (in cm^{-1}) for normalization.
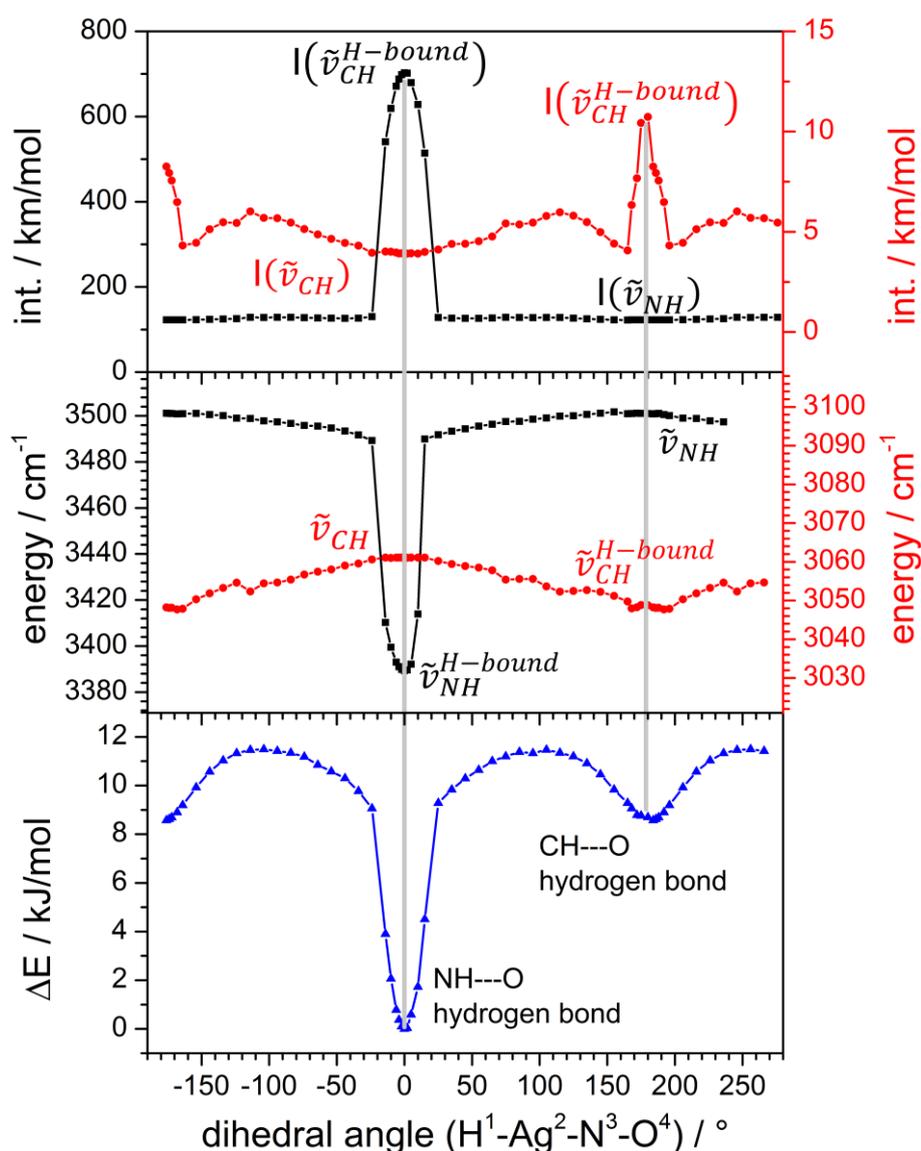
Figure 2): Total energy of torsional twisting in the $[AgL_1L_2]^+$ complex (bottom), frequencies of hydrogen bonding vibrations (middle) and their IR intensities (top) derived by DFT calculations at the B3LYP/cc-pVTZ (H, C, N, O) and Stuttgart 1997 RSC ECP (Ag) level of theory. Formation and breaking of the hydrogen bonds by torsional isomerization leaves marks in all three diagrams. Note that the angular width of the strong NH---O bond is narrow while that of the weaker CH---O bond is wider.
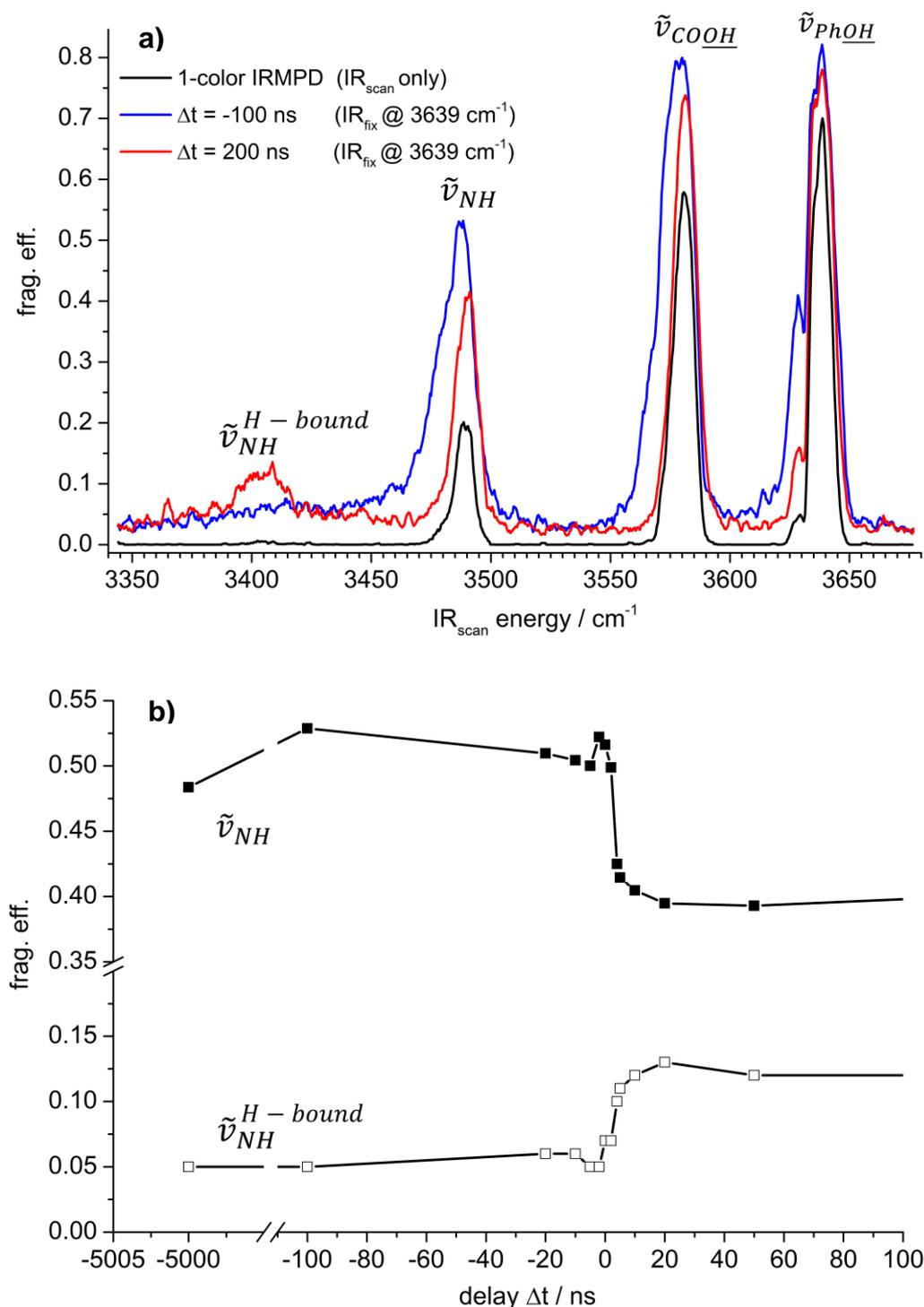
Figure 3a): Details from the infrared spectra of stretching vibrations in the $[AgL_1L_2]^+$ complex. The delay dependent two color IR-MPD spectra with selected time delay reveal heating effects and/or isomerization. **3b):** Fragmentation efficiency at the peak of the $\tilde{v}_{NH}$ band (filled squares) and the $\tilde{v}_{NH}^{H-bound}$ band (empty squares) in dependence of the time delay $\Delta t = t(IR_{fix}) - t(IR_{scan})$. A step like switch amongst both vibrations around $\Delta t = 0$ ns is clearly visible.